

# Fibronectin-modified surfaces for evaluating the influence of cell adhesion on sensitivity of leukemic cells to siRNA nanoparticles

**Aim:** This study aimed to create fibronectin (FN)-grafted polymeric surfaces to investigate the influence of leukemic cell adhesion on siRNA treatment. **Materials & methods:** FN was grafted on plasma-treated PTFE surfaces using chemical crosslinkers. Adhesion and growth of chronic myeloid leukemia K562 cells on modified surfaces were investigated. The silencing effect of siRNA/lipid-polymers nanoparticles on cells grown on FN-grafted surfaces was evaluated. **Results:** Crosslinker-mediated immobilization showed significant FN grafting on surfaces, which provided K562 cell adhesion and growth advantage. siRNA nanoparticle silencing was similarly effective on FN-adhered and suspension-growing K562 cells. **Conclusion:** This study provided initial data to develop a cell-adhesive system to investigate therapeutic effects on leukemic cells. The response of chronic myeloid leukemia cells to siRNA nanoparticles was independent on cell attachment.

First draft submitted: 29 September 2015; Accepted for publication: 11 February 2016; Published online: 13 April 2016

**Keywords:** biomaterial • cationic polymer • chronic myeloid leukemia • drug sensitivity • fibronectin • molecule grafting • polyethylenimine • siRNA delivery • surface modification • transfection

Chronic myeloid leukemia (CML) is initiated once the chromosomal translocation t(9;22) takes place in hematopoietic stem cells, giving rise to the constitutively active BCR-ABL oncogene. This oncogene is a tyrosine kinase that aberrantly triggers the activation of multiple proliferation and cell survival pathways, and promotes the progression of the disease. Current drug therapies are based on the use of tyrosine kinase inhibitors, which target CML cells that remain trapped in the cycling proliferative state. However, a proportion of the transformed cells could become insensitive to effect of these drugs mainly because they divide infrequently and remain in a quiescent state for weeks or even months [1,2]. The bone marrow microenvironment provides a niche that promotes cell-to-cell and cell-to-matrix interactions that are responsible for maintaining hematopoietic and progenitor

cells at quiescence and regulates their cellular renewal, differentiation and maintenance [1–4], so that molecular interactions in this niche can also dictate the fate of cells embedded in this niche [5]. Among the factors that contribute to engraftment of leukemic cells in bone marrow are extracellular matrix components, including fibronectin (FN) and collagen, soluble factors, such as stroma cell-derived factor (SDF-1), and stromal cells [3,4].

When leukemia develops, components of this environment can reduce the therapeutic effects of anticancer drugs and protect the cells against the drugs [1]. This is the case as well in CML, where the bone marrow anchored leukemic cells are known to display resistance to tyrosine kinase inhibitors (such as imatinib mesylate) and other chemotherapeutic drugs. This could explain, at least partially, why the full eradication of CML is not

Juliana Valencia-Serna<sup>1</sup>,  
Pascale Chevallier<sup>2</sup>, Remant  
Bahadur KC<sup>3</sup>, Gaétan  
Laroche<sup>2</sup> & Hasan Uludag<sup>\*1,3,4</sup>

<sup>1</sup>Department of Biomedical Engineering,  
Faculty of Medicine & Dentistry,  
University of Alberta, Edmonton, Alberta  
T6G 2V2, Canada

<sup>2</sup>Département de génie des mines, de la  
métallurgie et des Matériaux & Centre de  
recherche du CHU de Québec, Université  
Laval, Québec, Québec G1L 3L5, Canada

<sup>3</sup>Department of Chemical & Materials  
Engineering, Faculty of Engineering,  
University of Alberta, Edmonton, Alberta  
T6G 2G6, Canada

<sup>4</sup>Faculty of Pharmacy & Pharmaceutical  
Sciences, University of Alberta,  
Edmonton, Alberta T6G 2G6, Canada

\*Author for correspondence:

Tel.: +1 780 492 8809

Fax: +1 780 492 2881

[hasan.uludag@ualberta.ca](mailto:hasan.uludag@ualberta.ca)

Future  
Medicine part of

fsg

achieved in many cases [6]. To understand the means by which leukemic cells can bind to extracellular matrix components, Rainaldi *et al.* using flow cytometry and antibody staining, found that the cellular receptors for vitronectin, collagen and hyaluronan were not present on the cell surface of the widely used CML-model K562 cells, while the FN receptor (VLA-5;  $\alpha_5\beta_1$ ) was the only cell membrane receptor expressed on these cells [7]. This suggests that the adhesion of this type of leukemic cells to extracellular matrix occurs preferentially through the integrin-FN interactions. There is, therefore, a need to better understand the effects of particular interaction on the response of CML cells to current therapies.

Delivery of short interfering RNA (siRNA) against oncogenic targets is an emerging and promising therapy for management of CML. The siRNA therapy has the potential to silence the expression of virtually any gene of interest in leukemia and curb uncontrolled proliferation of leukemic cells [8]. We have developed nonviral siRNA nanoparticles that effectively deliver nucleic acids (i.e., siRNA) to suspension-growing leukemic cells and induce silencing of the expression of particular genes, such as the *BCR-ABL* oncogene [9]. As in other studies in the literature, our studies evaluated the efficacy of siRNA nanoparticles in suspension growing cells and no information exists on the response of adhered leukemic cells to siRNA therapy. Mimicking the bone marrow environment could be a valuable strategy for evaluating therapies that can promote the efficacy of emerging drugs in CML.

Toward this end, this study explored the modification of polytetrafluoroethylene (PTFE) films to make them more conducive for attachment of CML cells. We took advantage of the known role of FN in mediating attachment of CML cells to extracellular matrix, and created PTFE films with covalent grafting of FN and FN-derived CRGDS peptide. These types of modifications have been investigated previously in vascular grafts applications to promote endothelialization [10–12], but not to explore the attachment of leukemia cells and to evaluate the response to therapy under these conditions. In this study, the adhesion and growth of the CML model (K562 cells) on FN-grafted PTFE films was first explored. Next, the sensitivity to siRNA delivery was evaluated on the adhered leukemic cells and compared with the effect on the suspension-growing cells.

## Materials & methods

### Materials

The PTFE with a 250  $\mu\text{m}$  of thickness was purchased from Goodfellow Corp. (PA, USA) and sulfo-succinimidyl-4-(p-maleimidophenyl)butyrate (S-SMPB) from Life Technologies (ON, Canada). 5-Bromo-

salicylaldehyde, 1-ethyl-3-(3-dimethyl-aminopropyl) carbodiimide hydrochloride (EDC), MES buffer, glutaric anhydride (GA), bovine serum albumin, trypsin/EDTA, formaldehyde solution, hexamethyldisilazane, paraformaldehyde, spectroscopic grade dimethylsulfoxide and thiazolyl blue tetrazolium bromide (MTT) were purchased from Sigma-Aldrich (WI, USA). FN was acquired from ERRM (Université de Cergy-Pontoise, France). The CRGDS peptide (~600 g/mol) was purchased from Celtek Peptides (TN, USA). The rabbit primary polyclonal antibody anti-FN (F3648) was purchased from Sigma-Aldrich and the antirabbit IgG horseradish peroxidase-linked secondary (HRP-IgG) antibody was from Amersham/GE Healthcare BioSciences (NJ, USA). The Amplex® Red reagent was from Life Technologies. The RPMI Medium 1620 with L-glutamine, Dulbecco's Modified Eagle Medium (DMEM) F12, Hank's Balanced Salt Solution (HBSS; without phenol red), penicillin (10,000 U/ml solution), streptomycin (10,000  $\mu\text{g}/\text{ml}$ ) and heat-inactivated fetal bovine serum (FBS) were purchased from Invitrogen (NY, USA). Recombinant human basic FGF was obtained from the Biological Resource Branch of NCL-Frederickton (MD, USA). Coomassie brilliant blue was purchased from Bio-Rad (ON, Canada). The control (scrambled) siRNA was purchased from Invitrogen (ON, Canada). The GFP siRNA (GFP-22) was from Qiagen (ON, Canada).

### Polymeric siRNA carrier

A lipid-modified polymer, which consists of  $\alpha$ -linoleoyl chloride ( $\alpha\text{LA}$ ) grafted on low molecular weight ( $\text{MW} = 2.0 \text{ kDa}$ ) polyethyleneimine (PEI2) by N-acetylation (PEI2- $\alpha\text{LA}$ ), was used as the siRNA carrier and was prepared in house as follows:  $\alpha\text{LA}$  (2 mM) and PEI2 (1 mM) were dissolved separately in anhydrous chloroform and kept in ice for 30 min. Hundred microliters triethylamine were added to the PEI2 solution before it was mixed with the  $\alpha\text{LA}$  solution under stirring in ice. This mixture was then left stirring over night at room temperature. The crude product of PEI2- $\alpha\text{LA}$  was precipitated three-times in ice-cold diethyl ether and dried under vacuum for 2 days. The structural composition of PEI2- $\alpha\text{LA}$  was analyzed by  $^1\text{H}$ -NMR spectroscopy (Bruker 300 MHz, MA, USA) using tetramethylsilane as an internal standard in  $\text{D}_2\text{O}$  to calculate the lipid substitution levels. A substitution level of 2.72 lipids per PEI in PEI2- $\alpha\text{LA}$  was calculated based on this method.

### siRNA/polymer nanoparticles: preparation & characterization

The siRNA binding capacity of PEI2- $\alpha\text{LA}$  and native PEI2 polymers was elucidated by agarose gel retarda-

tion assay as described previously [13]. Briefly, 4  $\mu\text{l}$  of scrambled control siRNA (0.3  $\mu\text{g}/\mu\text{l}$ ) was diluted in NaCl (150 mM). Then, polymer solution (0.38  $\mu\text{g}/\mu\text{l}$ ) was added to the diluted siRNA solution to get final siRNA/polymer nanoparticle ratios ranging from 0 to 1:1. After a 30-min incubation at room temperature, nanoparticles were mixed with 4  $\mu\text{l}$  of loading dye (30% glycerol) and loaded onto agarose gel (0.8%, EtBr at 2  $\mu\text{g}/\text{ml}$ ) prepared in TAE buffer (1 $\times$ ). The gel was electrophoresed at 120 mV for 30 min. siRNA bands were visualized under UV (Alpha Imager EC).

The stability of the siRNA in polymer/siRNA nanoparticles was explored by serum digestion and quantified through gel retardation assay. Briefly, siRNA/polymer nanoparticles of ratio 1:5 (w/w) were prepared as described above. Then the nanoparticles were incubated with fetal bovine serum (final concentration 50% v/v) at 37°C for 24 h. The nuclease activity in serum was inactivated with 25 mM EDTA at 90°C for 15 min, and then the nanoparticles were dissembled with heparin (final concentration 50 U/ml) treatment for 1 h at room temperature. The crosslinked serum components were removed by centrifugation (2000 rpm, 5 min). Finally, the nanoparticles were electrophoresed as described above and the siRNA recovery was quantified.

Hydrodynamic size (*Z*-average) and surface charge ( $\zeta$ -potential) of the siRNA/polymer complexes (1:12 w/w) was assayed in ddH<sub>2</sub>O using dynamic light scattering and electrophoretic light scattering using Zetasizer Nano-ZS (Malvern, UK) equipped with He-Ne laser and operated at 10 mW.

### Preparation of PTFE films & surface functionalization with plasma treatment

The PTFE films (3  $\times$  3 cm) were washed successively with acetone, water and methanol in an ultrasonic bath for 10 min and air-wiped between steps. Clean PTFE films were stored under vacuum until use. X-ray photoelectron spectroscopy (XPS) analysis confirmed the efficiency of the cleaning procedure as the survey spectra revealed the presence of only carbon and fluorine in the appropriate stoichiometric ratio. For the surface modification with amine groups, PTFE films were placed on the grounded electrode of a parallel-plate dielectric barrier discharge reactor and treated in a gas environment containing 5% of H<sub>2</sub> and 95% of N<sub>2</sub>. The gas flow was introduced directly between the electrodes through a diffuser and was kept constant at 10 L/min. The mixture flowed through an oxygen trap (Restek, PA, USA) to nominally reduce the O<sub>2</sub> content of the gases to ppb levels. The frequency, gas, gap between electrodes and time were kept constant (3 kHz, 2 mm, 45 s), while the applied voltage was varied to ensure

that the same discharge power (or energy) was dissipated on the samples in the different atmospheric conditions ( $p = 0.25 \text{ W}/\text{cm}^2$ ,  $E = 15 \text{ J}/\text{cm}^2$ ).

The amine (NH<sub>2</sub>) surface concentration of plasma-treated PTFE films was quantified by vapor-phase chemical derivatization using 5-bromosalicylaldehyde followed by XPS analysis (below) to record survey spectra as described previously [14]. Taking into account the nine newly bounded atoms upon reaction of 5-bromosalicylaldehyde with the amino groups of the surface, the relative amine surface concentration was determined using the following equation: %NH<sub>2</sub> = [%Br/(100 – 9  $\times$  %Br)]  $\times$  100.

### Gluteraldehyde (GA) grafting on PTFE films

Plasma-treated PTFE films were immersed in a GA solution at 85 mg/ml under agitation. Fresh GA solution was added two more times 20 and 40 min after the beginning of the reaction. A total of 60 min after, the reaction was stopped and the films were successively washed and vortexed three-times with acetone and once with deionized water. The films were then air-wiped and kept under vacuum. Prior to FN grafting, carboxylic acid functionalities of GA-grafted PTFE films were activated with excess of EDCA in MES buffer (0.1 M, pH 4.75) under agitation and at room temperature. To avoid water-induced hydrolysis, EDCA was added three-times every 10 min. After 30 min of the reaction, the films were washed with MES buffer and used immediately for FN grafting [15].

### S-SMPB grafting on PTFE films

Plasma-treated PTFE films were individually covered with 600  $\mu\text{l}$  of 3 mg/ml S-SMPB (referred as SMPB from now on) in phosphate buffered saline (PBS) and incubated for 2 h at room temperature, under agitation and protected from light. The SMPB-grafted PTFE films were then rinsed in PBS, air-dried and used immediately for FN grafting (Protocol modified from [11]).

### FN & CRGDS peptide grafting on PTFE films

FN was purified from human plasma by a three-step combination of gelatin and heparin-cellulose affinity chromatography as described previously [16]. This protocol yielded a highly purified FN (>99.5%) devoid of blood plasma contaminants. The purified FN was filtered through a 0.2  $\mu\text{m}$  filter and stored at 8°C in 10 mM Tris buffer, pH 7.4. GA and SMPB modified PTFE films were reacted with 3  $\mu\text{g}/\text{ml}$  of FN in PBS 7.4 solution for 3 h under agitation at room temperature. After the reaction, the films were washed and vortexed five-times with PBS. For peptide grafting, PTFE films previously modified with SMPB were individu-

ally covered with 600  $\mu\text{l}$  of 20  $\mu\text{M}$  solution of CRGDS peptide in PBS and incubated for 3 h at room temperature (protocol adapted from [11]). Peptide-grafted films were then rinsed in PBS, air dried and stored under vacuum. A schematic representation of the chemical modifications performed on plasma-treated PTFE films is shown in Figure 1.

### XPS analysis

XPS analysis was performed at each step of the surface modification process. A PHU 5600-ci spectrometer (Physical Electronics, MN, USA) was used to record the spectra. A monochromatic aluminum X-ray source (1486.6 eV) at 300 W was used along with a charge neutralizer to record survey spectra while a monochromatic magnesium X-ray source (1253.6 eV) at 300 W was used to record high-resolution spectra. The detection angle was set at  $45^\circ$  with respect to the normal of

the surface. Three survey and high-resolution spectra were obtained for each sample.

### ELISA assay for bound FN

The untreated PTFE and treated PTFE films were subjected to ELISA analysis for FN quantitation. The films were placed in 96-well plates and blocked with 1% bovine serum albumin in PBS for 1 h at room temperature and rinsed once with PBS. The rabbit primary polyclonal antibody against FN (1:2500 dilution) was added on the films and incubated for 2 h at room temperature. After primary antibody was rinsed three-times with PBS, the antirabbit secondary antibody HRP-IgG was added at a dilution of 1:3000 and incubated for 2 h at room temperature. Films were rinsed three-times with Tris buffer and then transferred to new wells. Finally, 100  $\mu\text{l}$  of Amplex red solution (50  $\mu\text{M}$  containing 1 mM  $\text{H}_2\text{O}_2$ ) was added to

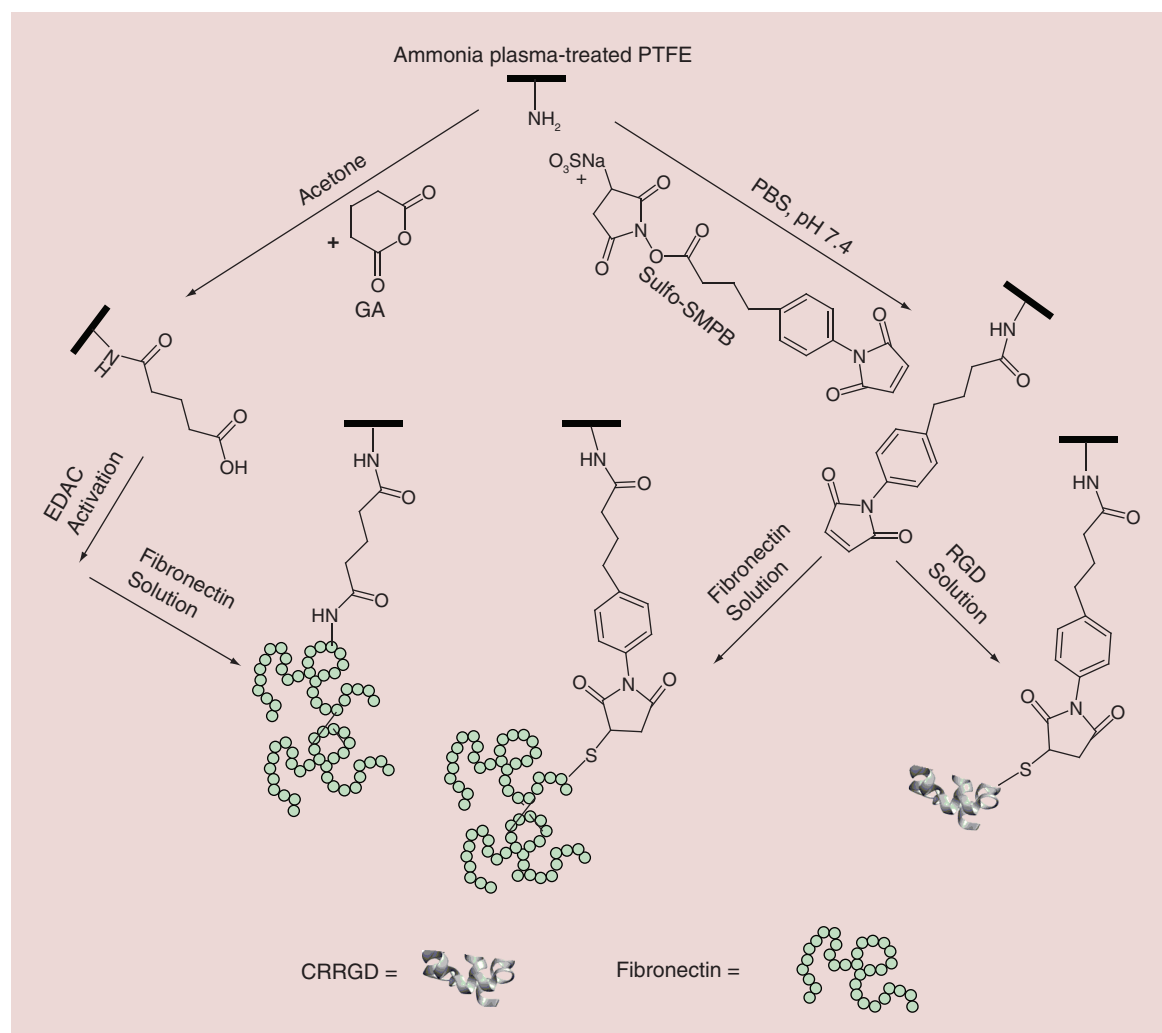


**Figure 1. Schematic representation of conjugation methods to covalently graft fibronectin or CRGDS molecules on plasma-treated modified PTFE films.** Two chemical crosslinkers were used for fibronectin grafting: GA (left) and sulfo-SMPB (right).



each film and incubated for 30 min in the dark at room temperature. A fixed amount of volume was transferred from each well to new wells and fluorescence intensity was read at 530/590 using a BioTek FL600 reader.

### Water contact angle

Static contact angle measurements were performed on the samples using a VCA 2500 XE system (AST, MA, USA). Drops of deionized water (1  $\mu$ l) were deposited on surfaces. At least three drops per samples and three samples per modification step were analyzed.

### Cell culture

K562 cells, which are derived from a *BCR-ABL* positive CML patient in blast crisis [17], were used as the CML model. A GFP-expressing K562 cell line (GFP-K562) was generated by transduction of K562 cells with a retroviral vector containing the green fluorescent protein (GFP) gene. GFP-K562 cells were kindly provided by Dr Xiaoyan Jiang (Terry Fox Laboratory, British Columbia Cancer Agency, Canada). GFP-K562 cells were used as the silencing model due to convenience of assessing GFP silencing. GFP-K562 cells were maintained in RPMI medium containing 10% FBS, 100 U/ml penicillin and 100  $\mu$ g/ml streptomycin under incubation at 37°C and 95% air/5% CO<sub>2</sub>. Twice per week, cells were diluted ten-times (1  $\times$  10<sup>6</sup> cells) in 20 ml of fresh medium for cell expansion or as noted for cell seeding.

Rat bone marrow stem cells (rBMSC) were isolated from both femurs of the female Sprague–Dawley rats (rats obtained from Biosciences; University of Alberta, Canada). The isolation protocol was described in detail previously [18]. rBMSC were maintained in culture with DMEM/F12 containing 10% FBS, 100 U/ml penicillin, 100  $\mu$ g/ml streptomycin, and supplemented with 5 ng/ml basic FGF under incubation at 37°C and 95% air/5% CO<sub>2</sub>. On confluence, the cells were trypsinized with 0.08% trypsin/0.04% EDTA, typically diluted four-times with the same medium and subcultured on 25 cm<sup>2</sup> flasks with 10 ml of fresh medium.

### Cell adhesion assay

The PTFE films were cut with a hole puncher (~6.4 mm diameter cylinders) and washed with sterile HBSS. In 96-well plates, 100,000 rBMSC or 15,000 K562 cells suspended in 100  $\mu$ l of respective media were seeded on PTFE films. After 1 day, unattached or loosely bound cells were removed with a HBSS wash, and attached cells were fixed with 3.7% (v/v) formaldehyde solution and then stained with 0.1% of coomassie brilliant blue. Staining solution was washed out with HBSS, and films were then transferred to new plates and imaged using a scanner Epson Perfection V550

Photo. As controls, unmodified PTFE, adsorbed FN (ads FN) on plasma-treated PTFE films (no cross-linker) and plasma-treated PTFE films with grafted GA (no FN) were used.

### SEM analysis

GFP-K562 cells suspended in 300  $\mu$ l of culture media (~2  $\times$  10<sup>5</sup> cells/ml) were seeded on PTFE films (11 mm of diameter) placed in 48-well plates. One day after cell adhesion, films were fixed overnight at 4°C with 2.5% glutaraldehyde, 2% paraformaldehyde in 0.1 M phosphate buffer and washed with 0.1 M phosphate buffer for 10 min ( $\times$ 3). For dehydration, films were immersed in aqueous solutions of increasing alcohol concentrations for 10 min, followed by immersion in aqueous solutions of decreasing alcohol and increasing hexamethyldisilazane concentrations for 10 min. Dry specimens were glued on SEM stubs and sputter coated with gold/palladium. SEM images were acquired using a Philips XL30 SEM (Microscopy Facility of the Department of Biological Sciences at the University of Alberta).

### MTT assay for cell growth

In 96-well plates, 10,000 K562 cells in 100  $\mu$ l of culture medium were seeded on the desired PTFE films. After 24 h of incubation, unattached cells were washed with HBSS and films were transferred to new wells. At desired time points (1, 5 and 7 days after cell seeding) MTT solution (5 mg/ml) was added to the wells to give a final concentration of 1 mg/ml and the cells were incubated for 1 h further, after which the medium was removed and the formed formazan crystals were dissolved with 100  $\mu$ l of dimethylsulfoxide. The PTFE films were removed from wells and the absorbance of the wells was measured with an ELx800 Universal Microplate Reader (BioTek Instruments, VT, USA) at 570 nm.

### Transfection of K562 cells with siRNA/lipid–polymer nanoparticles

The desired siRNAs and lipid-modified polymer (PEI2- $\alpha$ LA) were dissolved in nuclease-free water at 0.14 and 1  $\mu$ g/ $\mu$ l, respectively. For preparation of siRNA/lipid-polymer nanoparticles, siRNA solutions were first diluted in RPMI and the polymer solution were added to the diluted siRNA solutions. Solutions were mixed briefly with vortex and incubated for 30 min at room temperature to allow complex formation. RPMI medium alone (no complexes) was used for no treatment (NT) control groups, while Control (scrambled)-siRNA/lipid-polymer nanoparticles were used as negative controls. The siRNA:polymer (weight:weight) ratio was 1:12 and siRNA concentra-

tion in medium was 60 nM during cell treatments. The 1:12 siRNA:polymer ratio used corresponded to 48.6:1 N:P ratio (assuming 43.1 Da for single unit of PEI, 22 bp for siRNA with two phosphates per base pair). The effective polymeric carrier, optimal siRNA:polymer ratio and siRNA concentration were chosen based on previous studies using the same CML model [9].

For assessment of GFP silencing, GFP-K562 cells suspended in 300  $\mu$ l of culture media ( $1 \times 10^5$  cells/ml) were seeded on PTFE films (11 mm of diameter) in 48-well plates. Twenty-four hours after cell seeding (unattached cells were not removed), 100  $\mu$ l solutions containing GFP-siRNA/lipid-polymer nanoparticles were added to cells and incubated at 37°C. To take account for unspecific interactions of siRNA particles with films and siRNA effect on cells grown in suspension (positive control), cells growing in suspension in 48-well plates were similarly transfected with GFP-siRNA/lipid-polymer nanoparticles. Silencing effect of nanoparticles was evaluated by quantifying the reduction in GFP fluorescence in GFP-K562 cells of unattached (suspension growing) and attached cell fractions. For this, 4 days after transfection, cells growing in suspension were harvested and washed twice with HBSS by centrifugation (1400 rpm, 5 min) and, fixed in 3.7% formaldehyde solution. Cells attached to films were trypsinized, fixed and suspended in 3.7% formaldehyde solution. GFP silencing was assessed by flow cytometry (Cell Lab Quanta Sc., Beckman Coulter) using the FL-1 channel. Percent decrease in mean fluorescence was calculated as follows:  $100 - ([\text{Mean FL1 of cells treated with GFP siRNA/polymer}] / [\text{Mean FL1 of cells treated with scrambled siRNA/ polymer}] \times \%)$ .

For assessment of long-term GFP silencing in attached cells, GFP-K562 cells suspended in 300  $\mu$ l of culture media ( $1 \times 10^5$  cells/ml) were seeded on PTFE films (11 mm of diameter) in 48-well plates. A total of 24 h after cell seeding, unattached cells were removed with HBSS and the films were transferred to new wells. On day 5, fresh new media was added to cells. On day 7, spent media was removed, films were washed with HBSS, and 300  $\mu$ l of fresh media was added before 100  $\mu$ l solution containing GFP-siRNA/lipid-polymer nanoparticles were added to cells. For the cells grown in suspension, 300  $\mu$ l of  $1 \times 10^5$  cells/ml were transfected with 100  $\mu$ l solution containing GFP-siRNA/lipid-polymer nanoparticles. The GFP fluorescence in this assay was quantified by a plate reader (Assent, Thermo Scientific) at  $\lambda_{\text{EX}}$  and  $\lambda_{\text{EM}}$  of 485 nm and 527 nm, respectively. To quantify the GFP silencing, fluorescence values were normalized to the NT samples and the percent decrease in mean fluorescence was calculated as follows:  $100 - ([\text{Mean FL1 of cells treated}$

with GFP siRNA/polymer] / [Mean FL1 of cells treated with scrambled siRNA/ polymer]  $\times \%$ ).

### Statistical analysis

The data were summarized as the mean of the measured variables with the error bars representing one standard deviation. Where stated, the data between controls and treatment groups were analyzed for statistical difference by Student's *t*-test (two-tailed distribution and unequal variance). The level of significance was set at  $p < 0.05$ .

## Results & discussion

### siRNA/polymer nanoparticles characterization

Fraction of unbound siRNA was quantified to determine the binding capacity, which was based on  $BC_{50}$ ; in other words, siRNA/polymer ratio required for 50% siRNA binding. As expected, binding capacity of PEI2- $\alpha$ LA was less ( $BC_{50} = 0.25 \pm 0.01$ ) than native PEI2 ( $BC_{50} = 0.16 \pm 0.02$ ) (Figure 2A). This might be the consequence of primary amine consumption and steric hindrance generated by aliphatic chain. We have been observing this phenomena in our studies [13]. In the serum digestion studies, it was found that siRNA incubation in serum completely degrades the siRNA (as expected), and that the polymers (PEI2 and PEI2- $\alpha$ LA) were able to protect the encapsulated siRNA from the endonuclease activity of the serum (Figure 2B). Therefore, the polymer increased the stability of the siRNA under mimicked physiological conditions. Then hydrodynamic sizes of siRNA/polymer nanoparticles were assessed. As usual the size of siRNA/PEI2- $\alpha$ LA nanoparticles was significantly smaller ( $118.5 \pm 13.0$  nm) than the size of siRNA/PEI2 nanoparticles ( $712.4 \pm 17.9$  nm). It is believed that the lipid grafting enabled the shrinkage of the nanoparticles due to lipophilicity of the polymers (Figure 2C). Lipid grafting generally increases the surface charge of siRNA/polymer nanoparticles as the higher the grafting the higher the cationic charge density. The higher cationic charge density of siRNA/PEI2- $\alpha$ LA nanoparticles ( $38.8 \pm 2.6$  mV compared with  $31.9 \pm 0.7$  mV) might be consequence of smaller size which helps to concentrate the surface charge into a smaller surface area. These results are in agreement with our previous reports [13].

### FN grafting on aminated-PTFE films

For FN conjugation, PTFE films were first treated with  $N_2/H_2$  plasma to allow the addition of amine groups on their surface so that further chemical groups can be grafted. The covalent binding of FN on amine groups of PTFE films was realized by the GA and SMPB crosslinkers. These two crosslinkers were used as each

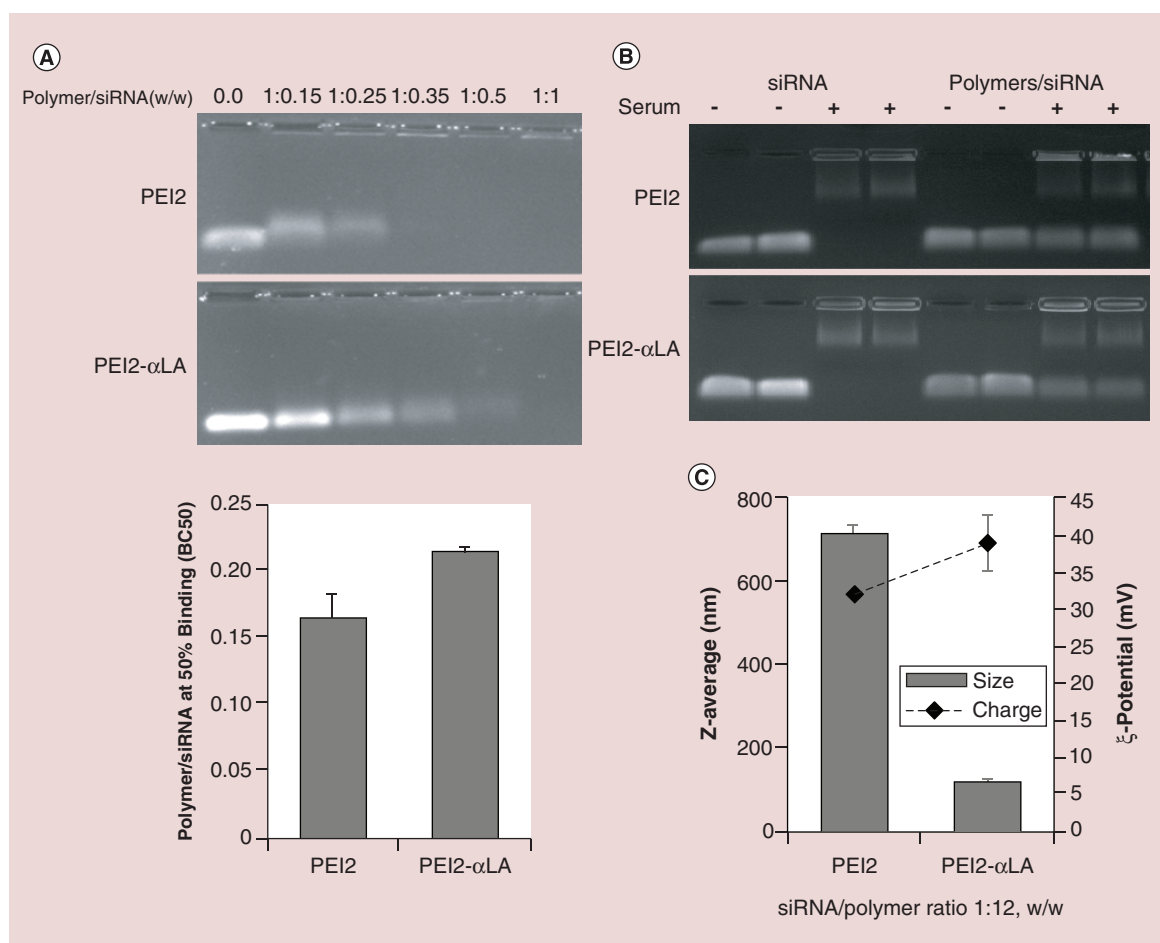


**Figure 2. Characterization of siRNA/polymer nanoparticles.** (A) siRNA binding capacity of PEI2 and PEI2-αLA as a function of siRNA/polymer weight ratio (top). BC50: siRNA/polymer weight ratio at 50% binding of PEI2 and PEI2-αLA (bottom). (B) Serum stability of siRNA/polymer nanoparticles of native PEI2 and PEI2-αLA. Recovery of intact siRNA from nanoparticles after 24 h exposure to 50% FBS at 37°C (by agarose gel electrophoresis). \* Serum background (not shown). (C) Size (nm) and surface charge of nanoparticles (siRNA/polymer = 1:12 w/w) prepared with PEI2 and PEI2-αLA.

one reacts with different sites of the FN molecule: the aldehyde groups of GA react with primary amines of FN, whereas the maleimide of SMPB can react with the thiol groups of FN. These two crosslinkers will therefore lead to different FN conformations and orientations on the surface, which may alter FN interactions with the cells [19]. To ensure that each chemical reaction took place, surface composition was assessed with XPS at each modification step (Table 1). Starting with the unmodified (clean) PTFE films, where the F/C ratio of 2 was expected, the films showed the addition of N and O components with a decrease in the percentage of fluorine after amination, indicating the proper fluorine etching and introduction of amines to PTFE surfaces. Moreover, the calculations derived from the chemical derivatization showed that plasma-treated PTFE films had relative amine surface percentages ranging from 3.4 to 6.5%. These amine

percentages are in agreement with previous studies [15]. After grafting of plasma-treated PTFE films with GA or SMPB, an increase in the percentage of O was seen due to the expected contributions of Os from the crosslinkers GA or SMPB.

Since no major changes were seen in the XPS-based atomic percentages when the FN was grafted to the films, an ELISA assay was subsequently performed to detect FN grafting, using PTFE (clean, no plasma) and plasma-treated PTFE films with adsorbed FN, and PTFE films where the FN was covalently bound with GA or SMPB (Figure 3). The negative controls, clean PTFE and PTFE+GA films, gave no detectable FN (background fluorescence), and a reasonable amount of FN was evident on FN-adsorbed clean PTFE films (no plasma treatment). The plasma treated PTFE films gave higher FN detection (compared with non-treated films), where the values in FN adsorbed and,

Table 1. Surface chemical composition assessed by XPS survey spectra for PTFE before and after each modification step. Plasma treatment (pt).

Element (%)	C	F	N	O
<b>Surface</b>				
Clean PTFE	31.8 ± 1.8	68.2 ± 1.8	-	-
Plasma-treated PTFE	54.0 ± 1.0	37.6 ± 0.9	6.1 ± 0.3	2.0 ± 0.4
PTFE + GA (with pt)	57.6 ± 1.4	27.3 ± 5.3	3.4 ± 0.3	11.2 ± 4.0
PTFE + SMPB (with pt)	64.2 ± 1.1	17.1 ± 1.9	6.1 ± 0.5	12.3 ± 1.9
PTFE + Ads FN (no pt)	55.6 ± 5.8	25 ± 3.6	6.3 ± 1.3	12.8 ± 0.9
PTFE + GA + FN	62.0 ± 1.8	18.6 ± 1.2	5.1 ± 0.6	14.1 ± 0.2
PTFE + SMPB + FN	62.7 ± 1.8	18.3 ± 1.7	6.5 ± 0.9	11.85 ± 1.8
PTFE + SMPB + CRGDS	63.6 ± 2.1	18.4 ± 2.9	5.9 ± 0.6	11.5 ± 0.4

GA and SMPB grafted FN surfaces were equivalent. These grafting efficiencies were consistent with previous studies [15].

Samples were tested by contact angle measurements to assess the hydrophobic/hydrophilic nature of different conditions. As shown in Table 2, the wettability for Clean PTFE surface was as expected  $127.9 \pm 2.1^\circ$  due to its hydrophobic nature, while the wettability of the plasma-treated PTFE with adsorbed FN (PTFE+Ads FN) was  $115.8 \pm 3.4^\circ$  and, of the plasma-treated PTFE with FN grafted with SMPB (PTFE+SMPB+FN) was  $75.7 \pm 2.3^\circ$ . Plasma treatment and FN adsorption increased slightly the hydrophilicity of the PTFE surfaces, while a more significant effect in hydrophilicity was recorded when the FN was grafted with SMPB crosslinker. These results indicated that modifying PTFE surfaces with plasma treated and grafting with FN increased substantially the hydrophilicity to make them more suitable for downstream evaluation.

It is known that FN is a highly flexible molecule, which undergoes conformational changes upon interaction with a surface. The conformational changes are dependent on the surface details and affect its biological activity [19,20]. PTFE (untreated) is a highly hydrophobic polymer and is often regarded as chemically inert, however its surface is not inert to protein adsorption under *in vitro* and *in vivo* conditions [21]. While non-specific FN adsorption can be significant on hydrophobic PTFE surfaces, as shown in Figure 3, other studies have shown that cell adhesive and growth abilities of adsorbed FN on hydrophobic surfaces was lower than that of the FN adsorbed on hydrophilic surfaces [21–23]. Upon contact with different surfaces, FN acquires a conformation that is dependent on the properties of the surface and, in the case of FN adsorbed on the hydrophobic PTFE, the FN conformation is thought to be in an inactive state due to inaccessibility of cell-binding regions to cellular adhesion receptors [21,22].

Amination of the PTFE surfaces with  $N_2/H_2$  plasma, on the other hand, reduces the surface hydrophobicity by introducing polar amine groups on the surface that will allow FN adsorption or chemical immobilization. Increased FN adsorption on plasma-treated PTFE films most likely took place through the electrostatic interactions between the introduced amino groups (cationic) with the negatively charged amino acids of FN (in addition to the hydrophobic interactions inherently existent with the PTFE surface). This type of binding is unspecific with random interaction along the protein chain and the protein should be in different conformations on the treated surface. FN grafting by covalent conjugation through either GA or SMPB is expected to be more stable and less prone to detachment [24]. Moreover, since the crosslinkers will bind to FN at specific sites, the grafted FN conformation and orientation on the surface is expected to be more uniform on the surfaces. Such differences in FN conformations upon FN adsorption or covalent grafting are bound to affect the biological activity of FN ultimately [25].

### Adhesion & growth of CML cells on FN-grafted PTFE films

FN-grafted PTFE films were tested for cell attachment with K562 cells as well as rBMSCs. The latter cells strongly depend on attachment for growth and were used as positive control for this cell adhesion experiment. Based on coomassie-blue stained cell mass in Figure 4, K562 and rBMSC cells appeared to show a similar adhesion pattern on the tested surfaces. The extent of cell attachment on Clean PTFE was almost negligible for both cell types. Cell adhesion on the films with adsorbed FN (PTFE+Ads FN) was sporadic and un-uniform with some variations in the attached cell mass among the replicates. The PTFE+GA films showed qualitatively similar cell attachment in com-



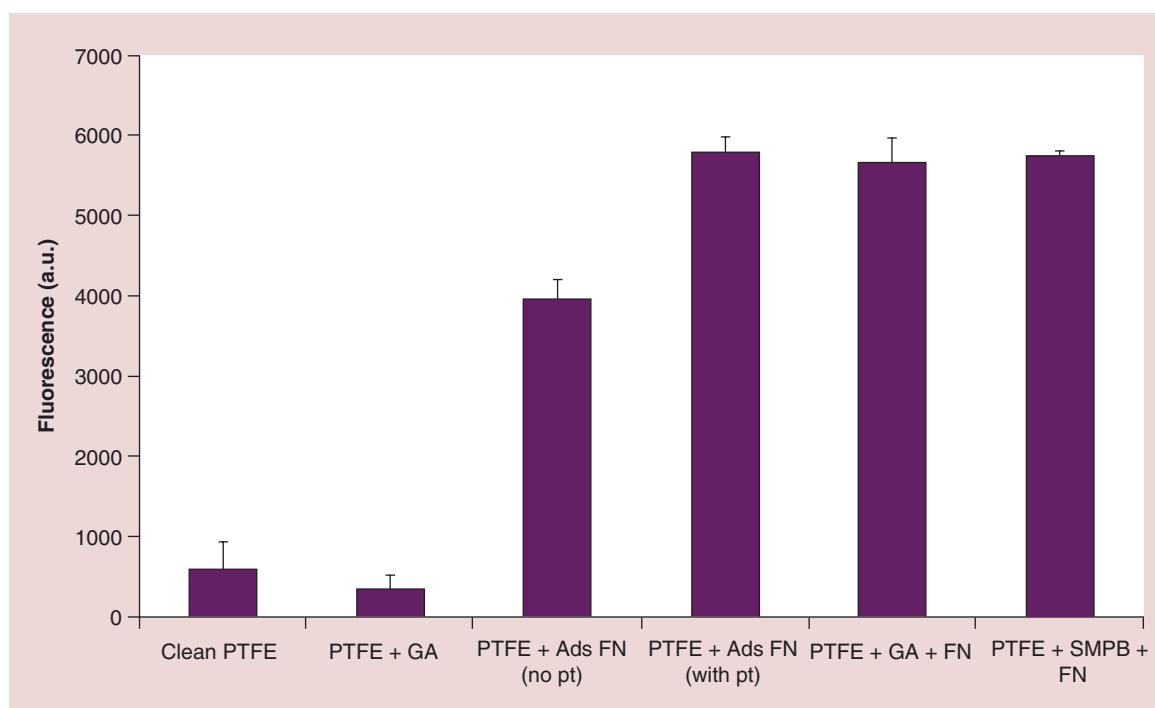


**Figure 3.** FN quantitation after FN was absorbed (Ads FN) on films untreated or treated with plasma (pt), or grafted on GA and SMPB modified PTFE films. Negative controls were unmodified (clean) PTFE films or GA-modified PTFE films. The FN was detected by ELISA assay using a polyclonal antibody against FN.

parison with adsorbed FN, while GA-grafted FN-PTFE (PTFE+GA+FN) films showed an increased cell density in comparison with PTFE+GA films, although not uniform among replicates. Grafting of FN with SMPB (PTFE+SMPB+FN films) allowed higher cell attachment of both rBMSC and K562 cells than the films where the grafting of FN was with GA (PTFE+GA+FN films). Moreover, grafting of RGD peptide with SMPB (PTFE+SMPB+CRGDS films) also showed high cell attachment and it was comparable with that of cell attachment to PTFE+SMPB+FN films.

Further analysis of K562 adhesion on modified PTFE films was performed by SEM (Figure 5). In accordance with the results above, there was no cell attachment on the Clean PTFE surfaces (Figure 5A), while cell densities on the PTFE+GA+FN, PTFE+SMPB+FN and PTFE+SMPB+CRGDS films were similar (Figure 5A). In the FN- or RGD-grafted cases, the cells appeared to interact with the films as it was evidenced by the presence of cytoplasmic projections coming out from the cells and microvilli that formed focal adhesions with the surfaces (Figure 5B). Moreover, some dif-

ferences in the cell morphology were noted among the films. For the case of the PTFE+GA+FN and PTFE+SMPB+CRGDS films (Figure 5B), cells were more cuboidal (3-dimensional) as projections from the cell bottom may be interacting with the surface, while for the PTFE+SMPB+FN films (Figure 5B), the cell morphology was flatter than the previous two surfaces, probably due to stronger interactions of the projections with the surface.

Growth of adhered K562 cells on modified PTFE films was evaluated on days 1, 5 and 7 after cell seeding based on the MTT assay (Figure 6A). The MTT absorbance values on day 1 for the PTFE+GA, PTFE+GA+FN, PTFE+Ads FN, PTFE+SMPB+FN and PTFE+SMPB+CRGDS films were higher than control films (Clean PTFE). The growth differences were noticeable among the treated films, where the growth was lower on the PTFE+GA+FN, and PTFE+Ads FN films, and higher for the last three groups, in which FN and peptides were covalently grafted with SMPB or GA (PTFE+GA+FN, PTFE+SMPB+FN and PTFE+SMPB+CRGDS). Moreover, in contrast to PTFE+GA+FN, cell

**Table 2.** Contact angle measurements. Mean  $\pm$  SD (n = 3).

Surface	Clean PTFE	PTFE+ Ads FN	PTFE + SMPB + FN
Contact angle	127.9 $\pm$ 2.1	115.8 $\pm$ 3.4	75.7 $\pm$ 2.3

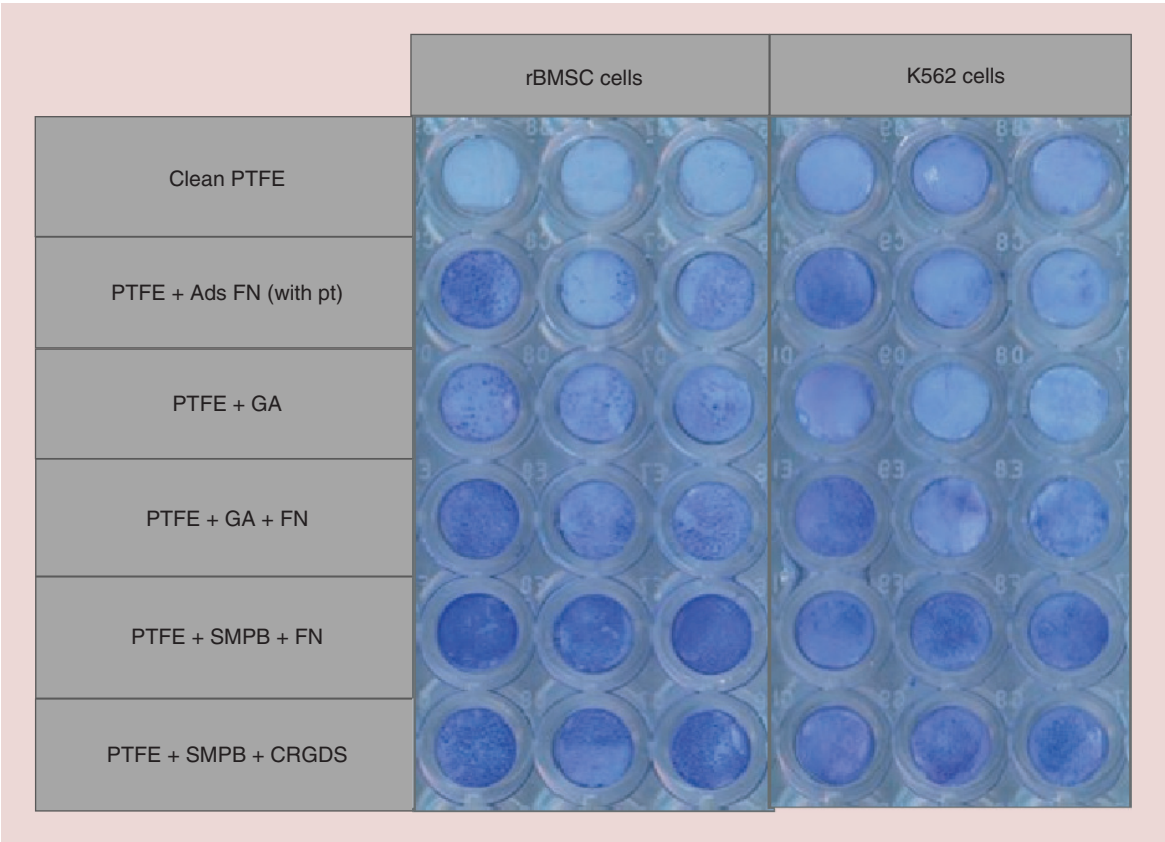


**Figure 4. Adhesion of anchorage-dependent rat bone marrow stem cells and nonanchorage dependent CML K562 cells on FN-modified PTFE films.** The mass of attached cells was visualized after Coomassie Blue staining. rBMSC: Rat bone marrow stem cell, pt: plasma treatment.

growth was more consistent and greater on the PTFE+SMPB+FN and PTFE+SMPB+CRGDS films, where the SMPB crosslinker was employed. This greater cell growth was evident by the significant difference ( $p < 0.05$ ) on day 5 for PTFE+SMPB+FN, and on days 5 and 7 for PTFE+SMPB+CRGDS films in comparison with Clean PTFE films. Based on the above results that show higher cell adhesion and growth of CML cells, the PTFE+SMPB+FN films were chosen for the remaining experiments of this study.

As a validation of the MTT-based growth results, coomassie blue staining was performed on K562 cells seeded on the PTFE+SMPB+FN and Clean PTFE films on days 2, 5 and 7 after cell seeding. **Figure 6B** shows the stained PTFE+SMPB+FN and Clean PTFE films with no cells (upper rows) and with seeded K562 cells (lower rows). The lack of staining on the films with no cells is evident for all days (upper rows), while on the Clean PTFE films where cells were seeded, there is no evidence of cell mass on day 2 and there are some sporadic traces of cell mass on days 5 and 7 (**Figure 6B**). In contrast, for the case of the PTFE+SMPB+FN where K562 cells were seeded, the cell mass is clearly evident starting from day 2 and it increased over day 7.

When Clean PTFE films are incubated with media containing 10% serum, they may be susceptible to unspecific protein adsorption and, serum FN may adsorb to surface and promote cell adhesion [22]. Studies analyzing the protein absorption on unmodified PTFE surfaces have found that the amount and type of bound proteins is what determine the cell attachment [21]. Our Clean PTFE films did not support cell adhesion initially, and it is likely that the amount of FN adsorbed on the hydrophobic surfaces is too small since albumin, the most abundant protein present in serum, will compete with FN for adsorption due to its preferential affinity to hydrophobic surfaces [22,26]. In PTFE+Ads FN films, there might be also a low amount of cell-binding inductive FN conformation with exposed cell binding sites [21,26]. Therefore, the small amount of FN adsorbed or low availability of cell-binding epitopes might not be sufficient for cellular binding [21]. The PTFE+GA films support a certain degree of cell adhesion and cell growth, similar to PTFE+Ads FN even though the PTFE+GA films do not have FN grafted. The increase of hydrophilicity after the plasma treatment may have allowed some FN adsorption from the serum that led a low degree of cell adhesion in this case.

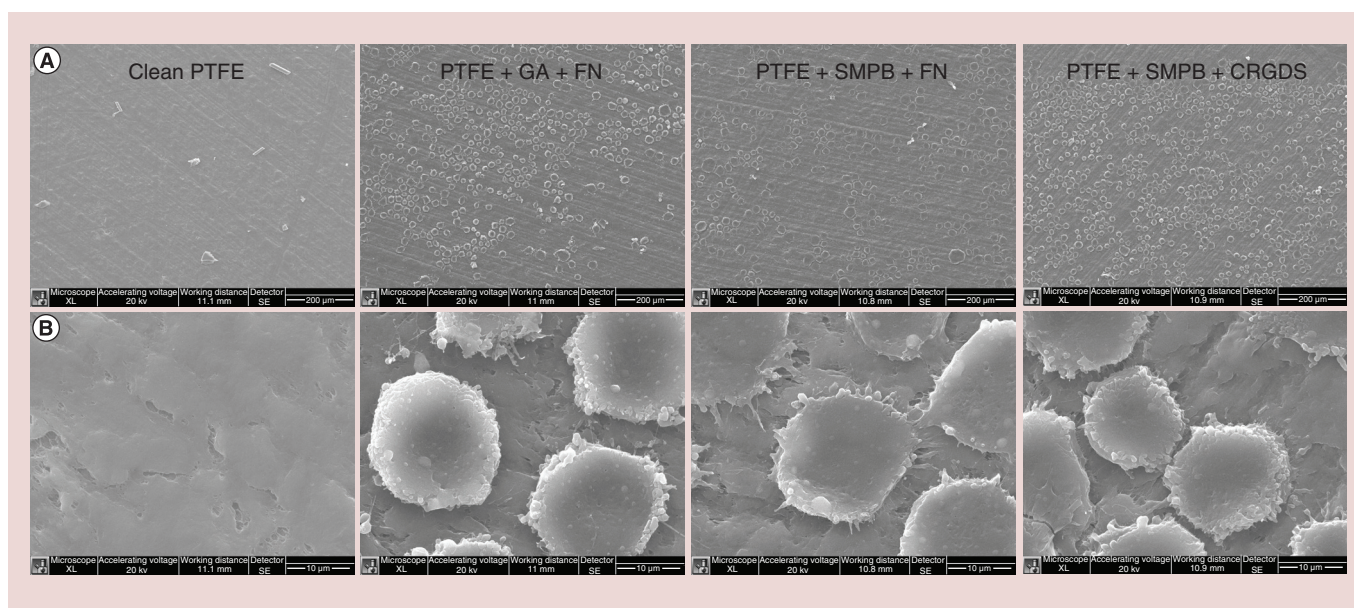


**Figure 5. SEM images of unmodified (clean PTFE) or FN- or RGD-grafted PTFE films. (A)** Wider field of view shows the cell density on the surface. **(B)** Closer field of view shows the interaction of cells (i.e., cellular projections) with the modified PTFE films where FN or CRGDS were covalently grafted with SMPB.

Regardless of the increased hydrophilicity after plasma treatment, uniform cell adhesion and robust cell growth was only possible to FN (and RGD) grafting. It was interesting to note that even the Clean PTFE surface had some sporadic growth on long-term studies. Such surfaces might be sufficiently ‘conditioned’ for cell growth with time, or ‘select’ specific population of cells for growth on this unique surface. Finding the reason(s) for this type of limited growth was considered

beyond the scope of this study, but it will be important to pursue for better understanding the response of sub-populations of CML cells.

#### Effect of GFP-siRNA transfection on GFP-positive cells adhered to FN-grafted PTFE films

To investigate the effect of siRNA transfection with lipid-modified polymers on cells adhered to FN-grafted films, silencing effect was assessed in GFP-K562 cells

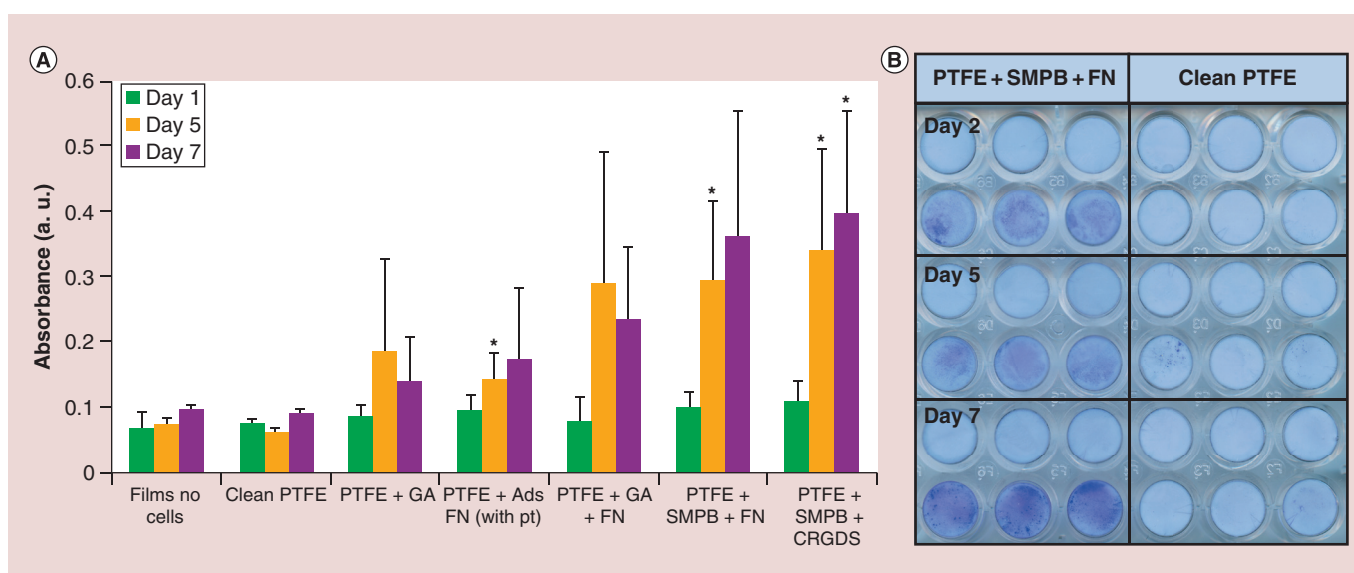


**Figure 6. Growth of adhered K562 cells on FN-modified PTFE films. (A)** Growth of K562 cells measured by the MTT assay on days 1, 5 and 7 after cell seeding. Significant difference in comparison with Clean PTFE films is indicated by \* $p < 0.05$ . **(B)** Mass of adhered K562 cells on PTFE+SMPB+FN and Clean PTFE films on days 2, 5 and 7 after cell seeding. Cells were stained with Coomassie Blue.



seeded on PTFE+SMPB+FN films. (PTFE+Ads FN films were not used in the transfection experiments because, as discussed above, cell adhesion on these films was not uniform among replicates, and showed slower cell growth in comparison with FN-grafted films). Cells seeded on FN-grafted PTFE films, Clean PTFE films and in suspension (no films) were transfected with GFP-siRNA/PEI2- $\alpha$ LA nanoparticles one day after seeding. Subsets of cells that did not attach to films and attached cells were analyzed four days after transfection. Specific GFP silencing is summarized as percentage of decrease in mean GFP fluorescence in **Figure 7A**. For the unattached cells (**Figure 7A**), when the cells were grown in suspension (no film), a GFP silencing of  $53.9 \pm 17.0\%$  was found, while for cells that grew on films unattached, the GFP silencing was  $33.0 \pm 6.6\%$  for Clean PTFE films and  $30.5 \pm 2.5\%$  for SMPB+FN films (**Figure 7A**). This was significantly lower than the case in the absence of films. This may suggest that the efficiency of the polymer/siRNA nanoparticles to interact with the suspension growing cells decreased due to the interaction of complexes with the PTFE surfaces. It may reflect a consequence of increased nanoparticle association with surfaces. The GFP silencing for cells attached to films (**Figure 7B**), was  $40.6 \pm 43.2\%$  for Clean PTFE and  $24.2 \pm 24.3\%$  for PTFE+SMPB+FN films (**Figure 7B**), indicating a similar level of silencing efficiency in this case. However, because the numbers of cells attached to the films were much lower than the numbers of cells growing unattached ( $\sim <1/3$ , not shown), the number of cells was suboptimal for flow cytometry analysis, which resulted in large error bars during the assessment of silencing for attached cells. The apparent contradiction of cells present in Clean PTFE films can be explained by the fact that few cells that were detected soon after cell seeding (**Figure 4**) could have increased their presence at longer incubation times (**Figure 6B**) due to a minimal adsorption of FN molecules of the serum-supplemented cell culture media on the Clean PTFE films. Also, since flow cytometry is more sensitive to the cell detection, these cells were more evident in this experiment than in previous assays. While a useful observation on the efficiency of siRNA nanoparticles on suspension growing cells was made in this experiment, we considered the short experimental period and subsequently low numbers of attached cells contributing to the large SDs in the outcome.

Cells were subsequently allowed to grow for a week on films prior to transfection with GFP-siRNA/PEI2- $\alpha$ LA nanoparticles. The GFP levels on the cells were assessed with a sensitive plate reader measurements four days after transfection since recovered cell numbers were again considered low for flow cytometry. The

results for suspension growing cells or cells attached on films (Clean PTFE and PTFE+SMPB+FN) are summarized in **Figure 8**. The GFP silencing of the cells grown in suspension (No Film) was  $36.4 \pm 9.0\%$ , whereas for the cells that grew attached to films, the GFP silencing for Clean PTFE films was  $7.6 \pm 3.5\%$  and for PTFE+SMPB+FN films was  $25.1 \pm 18.9\%$  (**Figure 8**). There is no significant difference between the GFP silencing of PTFE+SMPB+FN and No Film groups ( $p > 0.05$ ). Coomassie blue staining results four days after transfection confirm the presence of cells on PTFE+SMPB+FN films whereas only residual cells were present on Clean PTFE films (not shown). The lack of GFP silencing in Clean PTFE films was expected as only residual or no cells were found attached to these surfaces (**Figures 4 & 6B**). On the other hand, similar values of GFP silencing of cells attached via FN and cells in suspension may suggest that the transfection with the lipid-modified polymers is not affected by having cell attachment to surfaces.

### Other studies employing cell adhesive systems

Several studies have shown that adhesion of hematopoietic cell lines to FN provides a survival advantage to cytotoxic treatments in comparison with cells grown in suspension [27]. Cells that are vulnerable to treatment with different drugs, can become resistant to drugs once grown adhered to FN [6]. In the case of K562 cells adhered to FN, a reduced cell death was seen in comparison with cells in suspension after treatment with chemotherapy drugs imatinib mesylate and melphalan, and the  $\gamma$ -irradiation [27,28]. Previous studies suggested the underlying basis for the drug resistance is a crosstalk between the  $\beta_1$ -integrin signaling and the BCR-ABL kinase activity. Van der Kuip *et al.* suggested the possibility of PI3K pathway activation to prevent apoptosis [27]. This adhesion-mediated resistance was found to be reversible, as once the  $\beta_1$  integrin receptors were blocked by antibodies, the unattached cells became sensitive to drugs again. These studies suggest that there might be ways to make FN-adhered CML cells drug sensitive again, such as the disruption of the  $\beta_1$ -integrin mediated adhesion or downstream activators of the crosstalk with the BCR-ABL signaling. Reminiscent of siRNA-mediated silencing of BCR-ABL in K562 cells in previous studies, it might be useful to target adhesion receptors with nonviral siRNA delivery in order to reverse drug resistance. In contrast to reduced drug effects on FN-adhered CML cells, the GFP silencing by siRNA was not affected by the FN-mediated adhesion in this study, and it was comparable to GFP silencing efficiency in suspension cells.

Two other studies have delivered nucleic acids to adhered K562 cells. Yuan, *et al.* modified polycap-



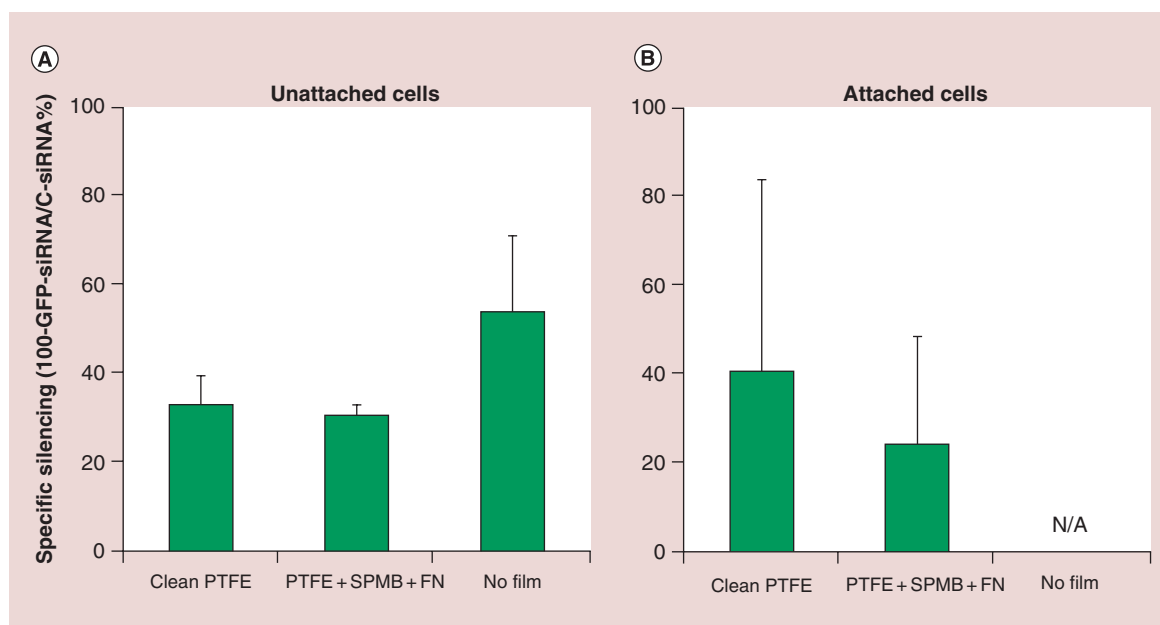


**Figure 7. GFP silencing after GFP-siRNA nanoparticle treatment on short-term cell growth.** One day after GFP-K562 cells were seeded on Clean PTFE, PTFE+SMPB+FN or in suspension (No Film), cells were treated with GFP-siRNA nanoparticles at 60 nM siRNA concentration (siRNA:polymer ratio of 1:12). Four days after transfection, GFP silencing (percent decrease in green fluorescence) was analyzed by flow cytometry of the cells unattached (A) and attached (B) to films. Large error bars in B are due to low cell numbers for optimal flow cytometry analysis. These results were from the average of three independent experiments.

lactone (PCL) films via surface-initiated atom transfer radical polymerization of poly(glycidyl methacrylate) (PGMA) to covalently immobilize gelatin [29]. The authors used these scaffolds to evaluate adhesion of K562 cells and transfection of cells with Lipofectamine 2000 complexes of plasmid DNA (not siRNA) [29]. K562 cells seeded on gelatin-functionalized PCL surfaces were able to adhere and proliferate while cells seeded on PCL did not proliferate. For the transfection studies, complexes were added on the scaffolds before or after cell seeding. The percentage of EGFP expression on transfected cells was slightly higher as compared with cells transfected on tissue culture plates: Percentage of EGFP-positive K562 cells was 7.4 and 4.7% on scaffolds and tissue culture plastic, respectively, while no transfection was observed on PCL [29]. The gene expression was not very efficient with this carrier, but no adverse effect of cell attachment on transfection was seen.

Another study from Hazlehurst *et al.* found that myeloma cells, which normally grow in suspension, displayed lower sensitivity to VP-16 drug once adhered to FN (6% apoptotic cells of FN-adhered cells vs. 30% of suspension cells) and that this resistance was reversed once FN adhesion was blocked by  $\beta$ 1 integrin antibodies (22% apoptotic cells). The authors found the FN-adhesion mediated resistance was associated with growth and cell cycle arrest that prevented drug-induced apoptosis. To investigate this, authors targeted

p27, a protein involved in impeding cell cycle progression, with antisense oligonucleotides (ASO) using a

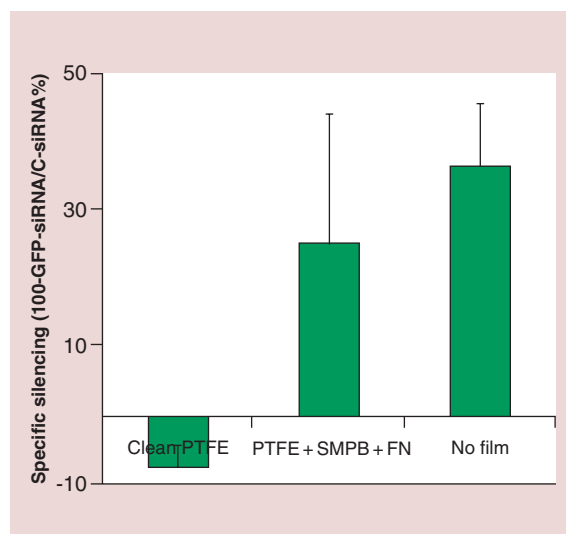


**Figure 8. GFP silencing after GFP-siRNA nanoparticle treatment on long-term cell growth.** One day after GFP-K562 cells were seeded on Clean PTFE, PTFE+SMPB+FN films and in suspension (no film), unattached cells were removed. One week after, cells were treated with GFP-siRNA nanoparticles at 60 nM siRNA concentration (siRNA:polymer ratio of 1:12). GFP silencing (percent decrease in green fluorescence) was calculated as described in the 'Materials & methods' section using a plate reader. These results are the average of three independent experiments.

commercial transfection reagent before and after FN adhesion of myeloma cells. After the treatment, a 75% reduction of p27 protein levels was found in comparison with cells treated with mismatch ASO. More importantly, although the cell adhesion to FN was not altered, the decrease of p27 protein restored the cell drug sensitivity, and the apoptosis induced by the VP-16 drug increased from 8.8% in mismatch ASO to 22% of cells treated with p27 ASO [4]. This study showed that inhibition of the cell cycle progression induced by FN adhesion via  $\beta 1$  integrins cell receptors can be reverted by silencing p27 protein. This therapeutic approach could be used for myeloma cells residing in the bone marrow that interact with FN so that these myeloma cells can be sensitized to the effect of pro-apoptotic drugs.

## Conclusion

The collective results of this study indicated that the nonattachment dependent CML K562 cells can be induced to attach and grow on engineered PTFE surfaces. Grafting the cell adhesive protein FN and its effective RGD epitope with SMPB were more efficient in promoting cell adhesion and subsequent growth on the films as compared with FN grafting via GA. Early cell adhesion to FN-modified films was the key to allow subsequent growth on films. Moreover, the GFP silencing induced by siRNA delivery with lipid-modified polymers can be similarly effective on FN-adhered K562 cells and cells grown in suspension. The SMPB-grafted

FN on PTFE films could be a viable model for assessing the effects of FN-mediated CML adhesion on siRNA responses. While specific targets for a therapeutic outcome remain to be investigated, this study provides the initial proof-of-principle data to develop a cell-adhesive system for leukemic cells. The proposed system could be useful to investigate the role of other extracellular matrix proteins and specific siRNA therapies to control undesirable leukemic growth.

## Acknowledgements

The authors would like to thank Andrée-Anne Guay-Bégin for her kind assistance in the vapor-phase chemical derivatization and film preparation.

## Financial & competing interests disclosure

This project was financially supported by operating grants from Alberta Innovates Health Solutions (AIHS), the Natural Sciences and Engineering Council of Canada (NSERC) and University of Alberta. In addition, J Valencia-Serna was supported by graduate studentships from NSERC CREATE Program of Regenerative Medicine (provided to G Laroche, Laval University) and Alberta Innovates Health Solutions. The authors have no other relevant affiliations or financial involvement with any organization or entity with a financial interest in or financial conflict with the subject matter or materials discussed in the manuscript apart from those disclosed.

No writing assistance was utilized in the production of this manuscript.

## Executive summary

### Background

- Leukemic cells can become insensitive to most drug therapies, allowing progression of the disease.
- Components of bone marrow environment, such as fibronectin (FN), are known to protect cells and reduce the therapeutic effect of anticancer drugs of leukemic cells.

### Aim

- This study explored the feasibility of creating a FN-grafted polymeric surface to investigate the influence of leukemic cell adhesion on siRNA treatment.

### Results

- FN covalently grafted with sulfo-succinimidyl-4-(p-maleimidophenyl)butyrate on plasma treated polytetrafluoroethylene films showed significant K562 cell adhesion and growth in comparison with unmodified surfaces.
- siRNA therapy using siRNA and lipid-modified polymer nanoparticles was similarly efficient on FN-adhered K562 cells and on K562 cells grown in suspension.

### Conclusion

- Lipid-modified polymers efficiently induced siRNA-mediating silencing on K562 cells regardless of whether they are in adhesion or suspension growth state.
- This study established the feasibility of developing a cell-adhesive system to test the influence of cell attachment on therapies.

## References

Papers of special note have been highlighted as: • of interest; •• of considerable interest

- 1 Wilson A, Trumpp A. Bone-marrow haematopoietic-stem-cell niches. *Nat. Rev. Immunol.* 6(2), 93–106 (2006).
- 2 Graham SM, Jørgensen HG, Allan E, Pearson C. Primitive, quiescent, Philadelphia-positive stem cells from patients with chronic myeloid leukemia are insensitive to ST1571 *in vitro*. *Blood* 99, 319–325 (2002).

- This study shows that quiescent hematopoietic stem cells

may survive the STI571 long-term monotherapy. They suggest the use of combinatory therapies to target this subset of cells.

- 3 Meads MB, Hazlehurst LA, Dalton WS. The bone marrow microenvironment as a tumor sanctuary and contributor to drug resistance. *Clin. Cancer Res.* 14(9), 2519–2526 (2008).
- **Review of the factors in bone marrow microenvironment that provides protection to hematopoietic cells from therapies. Soluble factors and cell adhesion that provides drug resistance environment, which are independent from epigenetic or genetic changes.**
- 4 Hazlehurst LA, Damiano JS, Buyuksal I, Pledger WJ, Dalton WS. Adhesion to fibronectin via  $\beta 1$  integrins regulates p27kip1 levels and contributes to cell adhesion mediated drug resistance (CAM-DR). *Oncogene* 19(38), 4319–4327 (2000).
- 5 Scadden DT. The stem cell niche in health and leukemic disease. *Best Pract. Res. Clin. Haematol.* 20(1), 19–27 (2007).
- 6 Hazlehurst LA, Dalton WS. Mechanisms associated with cell adhesion mediated drug resistance (CAM-DR) in hematopoietic malignancies. *Cancer Metastasis Rev.* 20(1), 43–50 (2001).
- 7 Rainaldi G, Filippini P, Ferrante A, Indovina PL, Santini MT. Fibronectin facilitates adhesion of K562 leukemic cells normally growing in suspension to cationic surfaces. *J. Biomed. Mater. Res.* 55(1), 104–113 (2001).
- 8 Landry B, Valencia Serna J, Gül-Uludağ H *et al.* Progress in RNAi-mediated molecular therapy of acute and chronic myeloid leukemia. *Mol. Ther. Nucleic Acids.* 4(5), e240 (2015).
- **Promising achievements of RNAi technology are discussed in leukemia with novel siRNA nanoparticles and challenges for this technology to be translated into clinics.**
- 9 Valencia Serna J, Gül-Uludağ H, Mahdipoor P, Jiang X, Uludağ H. Investigating siRNA delivery to chronic myeloid leukemia K562 cells with lipophilic polymers for therapeutic BCR-ABL down-regulation. *J. Control. Release* 172(2), 495–503 (2013).
- 10 Walluscheck KP, Steinhoff G, Kelm S. Improved endothelial cell attachment on ePTFE vascular grafts pretreated with synthetic RGD-containing peptides. *Eur. J. Vasc. Endovasc. Surg.* 12, 321–330 (1996).
- 11 Hoesli CA, Garnier A, Juneau P-M, Chevallier P, Duchesne C, Laroche G. A fluorophore-tagged RGD peptide to control endothelial cell adhesion to micropatterned surfaces. *Biomaterials* 35(3), 879–890 (2014).
- 12 Ren X, Feng Y, Guo J *et al.* Surface modification and endothelialization of biomaterials as potential scaffolds for vascular tissue engineering applications. *Chem. Soc. Rev.* 44, 5680–5742 (2015).
- 13 KC RB, Kucharski C, Uludağ H. Additive nanocomplexes of cationic lipopolymers for improved non-viral gene delivery to mesenchymal stem cells. *J. Mater. Chem. B* 3(19), 3972–3982 (2015).
- 14 Chevallier P, Castonguay M, Turgeon S, Ammonia RF-plasma on PTFE surfaces: chemical characterization of the species created on the surface by vapor-phase chemical derivatization. *J. Phys. Chem. B* 105(50), 12490–12497 (2001).
- 15 Vallières K, Petitclerc E, Laroche G. Covalent grafting of fibronectin onto plasma-treated PTFE: influence of the conjugation strategy on fibronectin biological activity. *Macromol. Biosci.* 7(5), 738–745 (2007).
- 16 Poulouin L, Gallet O, Rouahi M, Imhoff JM. Plasma fibronectin: three steps to purification and stability. *Protein Expr. Purif.* 17(1), 146–152 (1999).
- 17 Klein E, Ben-Bassat H, Neumann H *et al.* Properties of the K562 cell line, derived from a patient with chronic myeloid leukemia. *Int. J. Cancer* 18, 421–431 (1976).
- 18 Varkey M, Kucharski C, Haque T, Sebald W, Uludağ H. *In vitro* osteogenic response of rat bone marrow cells to bFGF and BMP-2 treatments. *Clin. Orthop. Relat. Res.* 443, 113–123 (2006).
- 19 Garcá AJ, Vega MD, Boettiger D. Modulation of cell proliferation and differentiation through substrate-dependent changes in fibronectin conformation. *Mol. Biol. Cell* 10, 785–798 (1999).
- 20 Ugarova TP, Zamarron C, Veklich Y *et al.* Conformational transitions in the cell binding domain of fibronectin. *Biochemistry* 34(13), 4457–4466 (1995).
- 21 Grainger DW, Pavon-Djavid G, Migonney V, Josefowicz M. Assessment of fibronectin conformation adsorbed to polytetrafluoroethylene surfaces from serum protein mixtures and correlation to support of cell attachment in culture. *J. Biomater. Sci. Polym. Ed.* 14(9), 973–988 (2003).
- 22 Grinnell F, Feld MK. Fibronectin adsorption on hydrophilic and hydrophobic surfaces detected by antibody binding and analyzed during cell adhesion in serum-containing medium. *J. Biol. Chem.* 257(9), 4888–4893 (1982).
- 23 Koenig AL, Gambillara V. Correlating fibronectin adsorption with endothelial cell adhesion and signaling on polymer substrates. *J. Biomed. Mater. Res. A.* 64(1), 30–37 (2003).
- 24 Zhang Y, Chai C, Jiang XS, Teoh SH, Leong KW. Fibronectin immobilized by covalent conjugation or physical adsorption shows different bioactivity on aminated-PET. *Mater. Sci. Eng. C* 27(2), 213–219 (2007).
- 25 Garcá AJ, Takagi J, Boettiger D. Two-stage activation for  $\alpha 5\beta 1$  Integrin binding to surface-adsorbed fibronectin. *J. Biol. Chem.* 273(52), 34710–34715 (1998).
- 26 Wei J, Igarashi T, Okumori N *et al.* Influence of surface wettability on competitive protein adsorption and initial attachment of osteoblasts. *Biomed Mater.* 4(4), 045002–045009 (2009).
- **This study shows that cross talk between integrin and BCR-ABL signaling pathways causes synergistic protection to apoptosis-inducing agents.**
- 27 van der Kuip H. Adhesion to fibronectin selectively protects Bcr-Abl+ cells from DNA damage-induced apoptosis. *Blood* 98(5), 1532–1541 (2001).
- 28 Damiano JS, Hazlehurst LA, Dalton WS. Cell adhesion-mediated drug resistance (CAM-DR) protects the K562 chronic myelogenous leukemia cell line from apoptosis induced by BCR/ABL inhibition, cytotoxic drugs, and  $\gamma$ -irradiation. *Leukemia* 15(8), 1232–1239 (2001).
- 29 Yuan W, Li C, Zhao C *et al.* Facilitation of gene transfection and cell adhesion by gelatin-functionalized PCL film surfaces. *Adv. Funct. Mater.* 22(9), 1835–1842 (2012).

